BIN2 phosphorylates the Thr280 of CO to restrict its function in promoting *Arabidopsis* flowering

Lan Ju[1†], Huixue Dong[2†], Ruizhen Yang[2†], Yexing Jing[2],
Yunwei Zhang[2], Liangyu Liu[3], Yingfang Zhu[4], Kun-Ming Chen[5],
Junai Ping[1*] and Jiaqiang Sun[2*]

[1]Shanxi Key Laboratory of Sorghum Genetic and Germplasm Innovation, Sorghum Research Institute,
Shanxi Agricultural University, Jinzhong, China, [2]National Key Facility for Crop Gene Resources and
Genetic Improvement, Institute of Crop Sciences, Chinese Academy of Agricultural Sciences,
Beijing, China, [3]Beijing Key Laboratory of Plant Gene Resources and Biotechnology for Carbon
Reduction and Environmental Improvement, and College of Life Sciences, Capital Normal University,
Beijing, China, [4]State Key Laboratory of Crop Stress Adaptation and Improvement, School of Life
Sciences, Henan University, Kaifeng, China, [5]State Key Laboratory of Crop Stress Biology in Arid Areas,
College of Life Sciences, Northwest A&F University, Yangling, China

CONSTANS (CO) is a central regulator of floral initiation in response to photoperiod. In this study, we show that the GSK3 kinase BIN2 physically interacts with CO and the gain-of-function mutant *bin2-1* displays late flowering phenotype through down-regulation of *FT* transcription. Genetic analyses show that BIN2 genetically acts upstream of CO in regulating flowering time. Further, we illustrate that BIN2 phosphorylates the Thr280 residue of CO. Importantly, the BIN2 phosphorylation of Thr280 residue restricts the function of CO in promoting flowering through affecting its DNA-binding activity. Moreover, we reveal that the N-terminal part of CO harboring the B-Box domain mediates the interaction of both CO-CO and BIN2-CO. We find that BIN2 inhibits the formation of CO dimer/oligomer. Taken together, this study reveals that BIN2 regulates flowering time through phosphorylating the Thr280 of CO and inhibiting the CO-CO interaction in *Arabidopsis*.

KEYWORDS

BIN2, CO, function, phosphorylation, flowering, *Arabidopsis*

Introduction

Flowering is a transition from the vegetative to the reproductive phase in the life cycle of flowering plants, which is controlled by several pathways, including photoperiod, autonomous, vernalization, age and gibberellin pathways (Andrés and Coupland, 2012). Among these pathways, photoperiod pathway plays a most important role in controlling *Arabidopsis thaliana* flowering time (Komeda, 2004). CONSTANS (CO) and FLOWERING LOCUS T (FT) are the central regulators of floral initiation in response to photoperiod (Putterill et al., 1995; Kobayashi et al., 1999). CO is a B-Box-type zinc finger transcription factor that promotes flowering by directly activating *FT* mRNA expression through binding to the two CO-responsive

elements (CORE1 and CORE2) in the *FT* promoter (Onouchi et al., 2000; Samach et al., 2000; Tiwari et al., 2010; Lv et al., 2021).

To date, several components have been identified to precisely regulate the diurnal transcription of *CO* in *Arabidopsis*. For example, CYCLING DOF FACTORs (CDFs) repress flowering by down-regulating *CO* transcription in the leaves (Sawa et al., 2007). The bHLH transcription factors FLOWERING BHLHs (FBHs) directly activate *CO* transcription to promote flowering (Ito et al., 2012). The TEOSINTE BRANCHED/CYCLOIDEA/PCF 4 (TCP4) transcription factor directly interacts with FBHs to synergistically activate *CO* transcription and promote flowering (Liu et al., 2017). A recent study reported that the histone demethylase JMJ28 regulates *CO* by interacting with FBH transcription factors to promote flowering (Hung et al., 2021). At the posttranscriptional level, the activity and stability of CO are also regulated. For example, NUCLEAR FACTOR Y (NF-Y) transcription factors physically interact with CO to activate *FT* expression in regulating flowering; TARGET OF EAT1 (TOE1) interacts with CO and inhibits its activity (Kumimoto et al., 2010; Zhang et al., 2015). In addition, CO can be ubiquitinated by CONSTITUTIVE PHOTOMORPHOGENIC1 (COP1) and degraded by 26S proteasome-dependent proteolysis (Jang et al., 2008; Liu et al., 2008). Interestingly, a previous study reported that CO can be phosphorylated, which contributes to the photoperiodic flowering response by facilitating the rate of CO degradation *via* the COP1 ubiquitin ligase (Sarid-Krebs et al., 2015).

Brassinosteroids (BRs) play a vital role in controlling floral transition. Previous studies have shown that BR biosynthetic and signaling mutants, including *de-etiolated 2* (*det2*), *constitutive photomorphogenesis dwarfism* (*cpd*), *brassinosteroid insensitive 1-1* (*bri1-1*) and *bin2-1*, display late-flowering phenotype (Li et al., 2002; Clouse, 2008; Li et al., 2010). However, the fundamental mechanism of BR-regulated flowering remains obscure. Up to now, BR signal transduction cascade from the cell surface receptor kinase BRI1 to the BRASSINAZOLE RESISTANT 1 (BZR1) family transcription factors has been well clarified (Wang et al., 2012; Chaiwanon et al., 2016). In the presence of BR, BRs bind to and activate BRI1, leading to inhibition of the GSK3-like kinase BRASSINOSTEROID INSENSITIVE 2 (BIN2) (Yan et al., 2009; Kim and Wang, 2010). Upon BIN2 inactivation by upstream BR signaling, BZR1 family transcription factors are dephosphorylated and accumulated in nuclear to regulate BR-responsive gene expression (He et al., 2002; Wang et al., 2002; Yin et al., 2002).

In this study, we demonstrate that BIN2 physically interacts with CO to phosphorylate its Thr280 residue, causing late flowering. On the other hand, we find that BIN2 prevents the formation of CO dimer/oligomer. Taken together, we uncover a regulatory module BIN2-CO in coordinating flowering time in *Arabidopsis*.

Materials and methods

Plant materials and growth conditions

Arabidopsis thaliana plants used in this study are in Col-0 ecotype background. The following mutants and transgenic lines used in the study have been previously described: *bri1-116* (Friedrichsen et al., 2000), *bin2-1* (Li and Nam, 2002), *det2-9* (Lv et al., 2018), *co-9* (Balasubramanian et al., 2006),, *35S:Flag-BIN2* (He et al., 2019). Seeds were grown on half-strength Murashige and Skoog medium and

stratified at 4°C for 2 d, then grown in long-day (16 h light/8 h dark) conditions at 22°C. Time-course analyses were performed on 14-d-old seedlings. *Nicotiana benthamiana* plants were grown under LD (16 h light/8 h dark) conditions at 24°C.

Analyses of flowering time phenotype

Analyses of flowering time were performed as previously described (Liu et al., 2017). Flowering time was scored as the number of days from germination to the first appearance of buds at the apex (days to bolting). More than 15 plants were counted and averaged for each measurement.

DNA constructs

For Gateway cloning, all the gene sequences were cloned into the entry vector *pQBV3* (Gateway) and subsequently introduced into certain destination vectors following the Gateway technology (Invitrogen) (He et al., 2019). For ligase-independent ligation, the ligation free cloning mastermix (abm) was used following the application handbook. For generation the mutant forms of *BIN2* and *CO*, their coding sequences were first cloned into the *pQBV3* vector, and then the point mutations were introduced by the specifically designed primers as previously described (Zheng et al., 2004), following the PCR amplification program: preheating at 94°C for 3 min, 16 cycles of 94°C for 1 min, 55°C for 1 min and 68°C for 4 min, finally, added DpnI and incubated at 37°C for 4 h. All details of DNA constructs and the primers used in this study are listed in Supplemental Table 1.

Generation of transgenic/hybrid plants

For the generation of *35S:YFP-CO* transgenic line, the full-length *CO* coding sequence was cloned into *p35S-YFP* vector to generate the *35S:YFP-CO* construct. The *35S:YFP-CO* construct was then transformed into the *Agrobacterium* strain *GV3101* and introduced into Col-0 by the floral-dip method (Clough and Bent, 1998). For the generation of *pCO : Flag-CO* and *pCO : Flag-CO*^{T280A} transgenic lines, the fragment containing the *CO* promoter and the *CO/CO*^{T280A} coding region were cloned into the *pCAMBIA1301* vector to generate the *pCO : Flag-CO* and *pCO : Flag-CO*^{T280A} constructs, respectively. Then the *pCO : Flag-CO* and *pCO : Flag-CO*^{T280A} constructs were transformed into the *Agrobacterium* strain *GV3101* and introduced into the *co-9* mutant background by the floral-dip method.

The *35S:YFP-CO/bin2-1* line was generated through genetic crossing between the *35S:YFP-CO* and *bin2-1* lines. The *35S:YFP-CO/35S:Flag-BIN2* double transgenic plants were generated by genetic crossing between the *35S:YFP-CO* and *35S:Flag-BIN2* transgenic lines.

RNA extraction and quantitative real-time PCR

Total RNAs were extracted using a plant total RNA extraction kit (Zoman). Total RNA concentration was measured by Nanodrop 2000

(Thermo Fisher Scientific NanoDrop). About 2 μg of total RNA was used for reverse-transcribing to cDNA by abm reverse transcriptase kit. The cDNA was diluted to 100 μL with water in a 1:5 ratio, 2μL diluted cDNA was used for qRT-PCR. And qRT-PCR was performed with SYBR Premix Ex Taq (TaKaRa) on Light Cycler 96p (Roche). *ACTIN7* was used as an internal control. Experiments were performed independently three times with similar results. All the primers used for qRT-PCR are listed in Supplemental Table 1.

LCI assays

The LCI assays were performed in *N.benthamiana* leaves as described previously (He et al., 2019; Yang et al., 2021). Briefly, the full-length or truncated forms of the genes were cloned into the *pCAMBIA1300-nLUC* and *pCAMBIA1300-cLUC* vectors. Different constructs were transformed into the *Agrobacterium* strain *GV3101* and then co-infiltrated into *N. benthamiana* leaves. Then plants were incubated for 12 h under dark and 36 h under light, and the LUC activities were analyzed using NightSHADE LB985 (Berthold). For each protein-protein interaction assay, at least 5 independent *N. benthamiana* leaves were infiltrated and analyzed, and 3 independent biological replications were performed for each assay (Sun et al., 2013).

Yeast two-hybrid assays

For yeast two-hybrid (Y2H) analysis, the full-length or truncated forms of the genes were cloned into vectors *pGADT7* or *pGBKT7*, respectively. Different constructs were transformed into *AH109* yeast cells, and grown on agar plates with SD–L/W (synthetic dextrose medium lacking Leu and Trp). Further, the yeast cells were screened on SD–L/W/H medium (synthetic dextrose medium lacking Leu, Trp and His). Plates were kept at 30°C for 3 to 4 days. The empty vectors *pGADT7* and *pGBKT7* were used as negative controls.

Co-IP assays

For the co-immunoprecipitation (Co-IP) assays, the *35S:YFP-CO* and *35S:YFP-CO/35S:Flag-BIN2* transgenic plants were used for detecting the interaction between CO and BIN2. Samples were harvested at ZT16 and then grounded to fine powder in liquid nitrogen. The total proteins were extracted by the lysis buffer (50 mM Tris-HCl at pH 7.5, 150 mM NaCl, 5 mM EDTA at pH 8.0, 0.1% Triton X-100, 0.2% NP-40) with freshly added PMSF (phenylmethylsulphonyl fluoride, 10 mM), Roche protease inhibitor cocktail (Roche, 11873580001) and MG132 (20 μM). After centrifugating at 4°C for 20 min, Extracts were mixed with Protein-G (Invitrogen, 00621751) for 1 h to reduce nonspecific immunoglobulin binding, and then incubated with anti-GFP magnetic beads (MBL, M047-8) overnight at 4°C. The precipitated samples were washed at least five times using the lysis buffer and then added 2X SDS protein loading buffer boiling for 5 min. The beads were detected by anti-GFP

(1:2000; Roche, 11814460001) and anti-Flag (1:5000; abmart, M20026) antibodies.

In vitro pull-down assays

The full-length coding sequences of CO and BIN2 were cloned into the *pGEX4T-1* and *pMAL2X-1* vectors to generate GST-CO and MBP-BIN2, respectively. These fusion proteins were expressed and purified from *E. coli* strain *Transetta-DE3* (Transgen biotech, CD801). The pull-down assays were performed as described previously (Yang et al., 2021). For the assay, prewashed amylose resin in the column buffer (20 mM Tris [pH 8.0], mM NaCl, 1 mM EDTA) was used to pull down protein complexes. The mixture with proteins and amylose resin was incubated overnight at 4°C, then washed for 5 times with wash buffer, and added 2X SDS protein loading buffer boiling for 5 min. Eluted proteins were analyzed by immunoblotting using anti-MBP (1:3000; CWBIO, CW0288) and anti-GST (1:3000; CWBIO, CW0144) antibodies.

Protein extraction and immunoblotting

For protein level analysis, every 100 mg of *Arabidopsis* seedlings or *N. benthamiana* leaves added 200 μl protein extraction buffers. The extracted buffer used for extracting plants is described previously (He et al., 2019; Yang et al., 2021). The supernatant was separated on SDS-PAGE gels, and transferred to polyvinylidene fluoride membranes. For the protein detection, anti-Flag (1:5000; abmart, M20026) were used to detect Flag-CO proteins. Anti-Actin (1:5000; CWbiotech, CW0264) was used as a loading control.

In vitro phosphorylation assay

For Phosphorylation assay, 1 μg BIN2-MBP/MBP and 1 μg CO-GST/mutated CO fusion proteins were added into kinase reaction buffer (25 mM Tris at pH 7.4, 12 mM MgCl$_2$, 1 mM DTT, and 1 mM ATP). Then the mixture was incubated at 37°C for 1 h and boiled with 5×SDS loading buffer. The boiled reaction products were separated by SDS-PAGE with or without 50 μM Phos-Tag (NARD, AAL-107). The phosphorylated CO was detected with anti-GST antibody.

Chromatin immunoprecipitation-qPCR assay

The ChIP assays were carried out following a published protocol (Liu et al., 2017). *Arabidopsis* seedlings were grown on ½ MS for 10 d, 1.5g materials were collected and crosslinked in crosslinking buffer, then their chromatin was isolated. Anti-Flag ChIP grade antibody (ABclonal, AE005) and protein G plus agarose were used to immunoprecipitate the protein–DNA complex. Finally, the Flag-specific enrichment of the fragments from *FT* promoter was

analyzed by qPCR using specific primer sets listed in Table S1. The enrichment fold of a certain fragment was calculated by normalizing to the amount of no antibody-immunoprecipitate DNA samples.

Subcellular localization assays

The coding sequences of CO, CO^{T280A}and Q were cloned into the *pEarly-101* vector to generate YFP-CO, YFP-CO^{T280A} and mCherry-Q constructs, respectively. Then the constructs were transformed into the *Agrobacterium* strain *GV3101* and infiltrated into *N. benthamiana* leaves. The fluorescence signal of yellow fluorescent protein (YFP) was observed at 48 h post-infiltration.

Accession numbers

Sequence data in *Arabidopsis* from this study can be found in the *Arabidopsis* Genome Initiative database under the following accession numbers: *BRI1* (AT4G39400), *DET2* (AT2G38050), *BIN2* (AT4G18710), *CO* (AT5G15840), *FT* (AT1G65480) and *ACTIN7* (AT5G09810), *SK12*(AT3G05840), *SnRK2.6*(AT4G33950), *MPK6*(AT2G43790).

Results

BIN2 physically interacts with CO

CONSTANS (CO) is a central regulator of floral initiation in response to photoperiod. In order to explore the regulatory effects of phosphorylation and specific protein kinases for CO, we tested a series of kinases for CO interaction through the luciferase (LUC) complementation imaging (LCI) assay. In the LCI assay, CO was fused with the amino-terminal part of LUC (nLUC) and kinases (BIN2, SK12, SnRK2.6 and MPK6) were ligated to the carboxyl-terminal part of LUC (cLUC) to generate nLUC-CO and cLUC-BIN2 (SK12, SnRK2.6, MPK6), respectively. The results showed that strong LUC activity could be observed when nLUC-CO/cLUC-BIN2 and nLUC-CO/cLUC-SK12 were co-expressed in *Nicotiana benthamiana* leaves, but no LUC activity was detected in nLUC-CO/cLUC-SnRK2.6, nLUC-CO/cLUC-MPK6 (Figure 1A). Since BIN2 and SK12 (a homolog of BIN2) interact with CO, we further tested the interaction between BIN2 and CO through other approaches. In the yeast two-hybrid (Y2H) assay, BIN2 was fused with *pGBKT7* and CO was ligated to *pGADT7* to generate BD-BIN2 and AD-CO, respectively. The *AH109* strain yeast cells transformed with BD-BIN2 and AD-CO could grow well in the selection medium, but
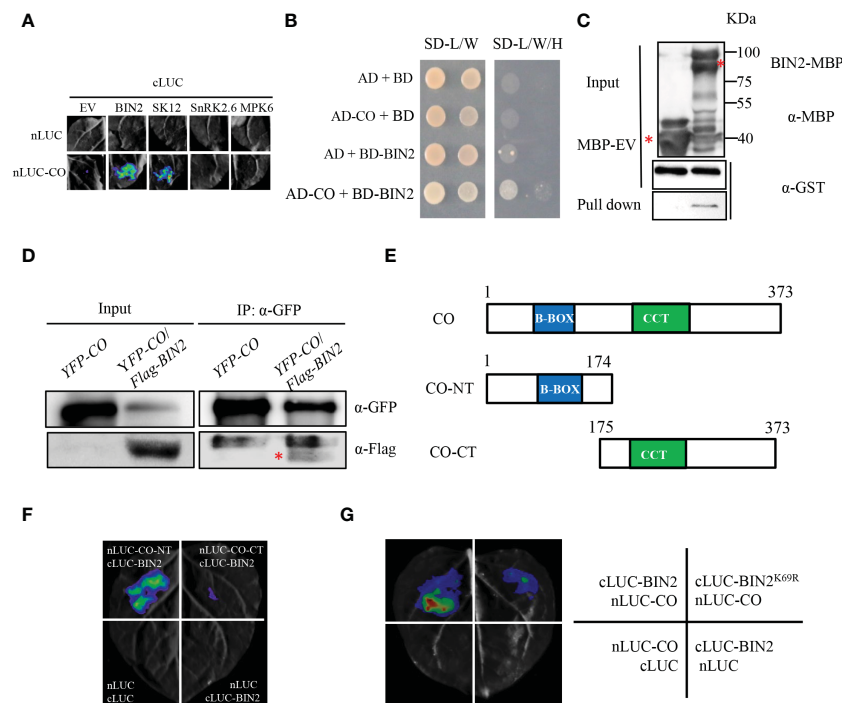

FIGURE 1

BIN2 physically interacts with CO *in vitro* and *in vivo*. **(A)** Identification of CO-interacting protein kinases. Luciferase complementation imaging (LCI) assays showing the interactions between CO and protein kinases in *N. benthamiana* leaves. Representative images of *N. benthamiana* leaves after infiltration were shown. Empty vectors were used as negative controls. **(B)** Y2H assay showing the interaction between BIN2 and CO. SD-L/W, synthetic dextrose medium lacking Leu and Trp; SD-L/W/H, synthetic dextrose medium lacking Leu, Trp and His. **(C)** *In vitro* pull-down assay showing that BIN2 directly interacts with CO. Purified GST-CO proteins were incubated with MBP or MBP-BIN2 for the MBP pull-down assay. Red asterisk indicates specific bands. **(D)** Co-IP assays showing the interaction between BIN2 and CO in *Arabidopsis*. The *35S:YFP-CO* and *35S:YFP-CO/35S:Flag-BIN2* transgenic plants were grown for 10 days under LDs. Red asterisk indicates specific signal. The immunoprecipitates were detected using anti-GFP and anti-Flag antibodies, respectively. **(E)** Schemes displaying full-length and truncated versions of the CO protein. CO-NT, amino terminal domain of CO; CO-CT, carboxyl terminal domain of CO. **(F)** LCI assay showing the interaction between the truncated versions of CO and full-length BIN2 in *N. benthamiana* leaves. **(G)** LCI assay showing less LUC activities between BIN2^{K69R} and CO.

the negative controls did not (Figure 1B), indicating that BIN2 physically interacts with CO in yeast cells. Consistently, the MBP-BIN2 fusion proteins could retain GST-CO proteins, whereas MBP alone could not, indicating that BIN2 directly interacts with CO in the *in vitro* pull-down assay (Figure 1C). Moreover, we generated the *35S: Flag-BIN2/35S:YFP-CO* double transgenic plant through genetic crossing between the *35S:Flag-BIN2* and *35S:YFP-CO* lines for the Co-IP assay. The results showed that the Flag-BIN2 proteins could be precipitated by YFP-CO proteins in the double transgenic *35S:Flag-BIN2/35S:YFP-CO* seedlings in the Co-IP assay, further suggesting that BIN2 interacts with CO *in vivo* (Figure 1D).

To map the interaction region of CO with BIN2, the full-length of CO protein was truncated into N-terminal part harboring the B-Box domain (CO-NT) and C-terminal part containing the CCT domain (CO-CT) (Figure 1E). Those two parts of CO were fused with nLUC to generate nLUC-CO-NT and nLUC-CO-CT for LCI assays, respectively. As shown in Figure 1F, obvious LUC activities were observed in the nLUC-CO-NT/cLUC-BIN2 co-expression samples, but only background level of LUC activities was observed in the nLUC-CO-CT/cLUC-BIN2 samples. These results suggest that the N-terminal part of CO containing the B-Box domain is required for the interaction with BIN2 (Figure 1F). Moreover, we also explored whether the kinase activity of BIN2 is required for its interaction with CO. BIN2^{K69R} mutant form, in which the Lys69 was replaced by Arg and the GSK kinase activity was abolished, was fused with cLUC to generate cLUC-BIN2^{K69R} for LCI assays. As shown in Figure 1G, less LUC activities were detected in the cLUC-BIN2^{K69R}/nLUC-CO co-expression samples than those in the cLUC-BIN2/nLUC-CO co-expression samples (Figure 1G), suggesting that the kinase activity of BIN2 is essential for its interaction with CO.

Since BIN2 physically interacts with CO, we were curious whether these two genes have similar expression patterns during photoperiod. To address this question, we analyzed the expression patterns of *BIN2* and *CO* in Col-0 during a 24-h photoperiod. Interestingly, we found that the transcripts of *BIN2* exhibited similar diurnal expression patterns with *CO* (Supplementary Figure 1), supporting the notion that BIN2 is supposed to post-transcriptionally modify CO protein in regulating flowering time.

BIN2 regulates flowering time genetically upstream of CO

Although it has been known that BRs play an important role in promoting flowering in *Arabidopsis*, the underlying mechanism remains largely unclear. To explore the biological role of BR pathway in regulating flowering time, we systematically examined the flowering time phenotypes of BR biosynthetic and signaling mutants including *bin2-1*, *det2-9* and *bri1-116* under LD (16 h light/8 h dark) conditions. The results showed that *bin2-1*, *det2-9* and *bri1-116* displayed obvious late-flowering phenotypes compared with the wild type (WT) Columbia-0 (Col-0) under LD conditions (Figures 2A, B and Supplementary Figures S2A, B). To further dissect the molecular effect contributing to the late flowering of BR biosynthetic or signaling mutants, we analyzed daily expression patterns of *FT*, a key integrator of flowering time (Putterill et al., 1995; Kobayashi et al., 1999), in these mutants using quantitative RT-PCR (qRT-PCR). The qRT-PCR assays revealed that the expression levels of *FT* in Col-0 plants were peaked at Zeitgeber time 16 (ZT16), consistent with previous report (Turck et al., 2008), but the peak of *FT*
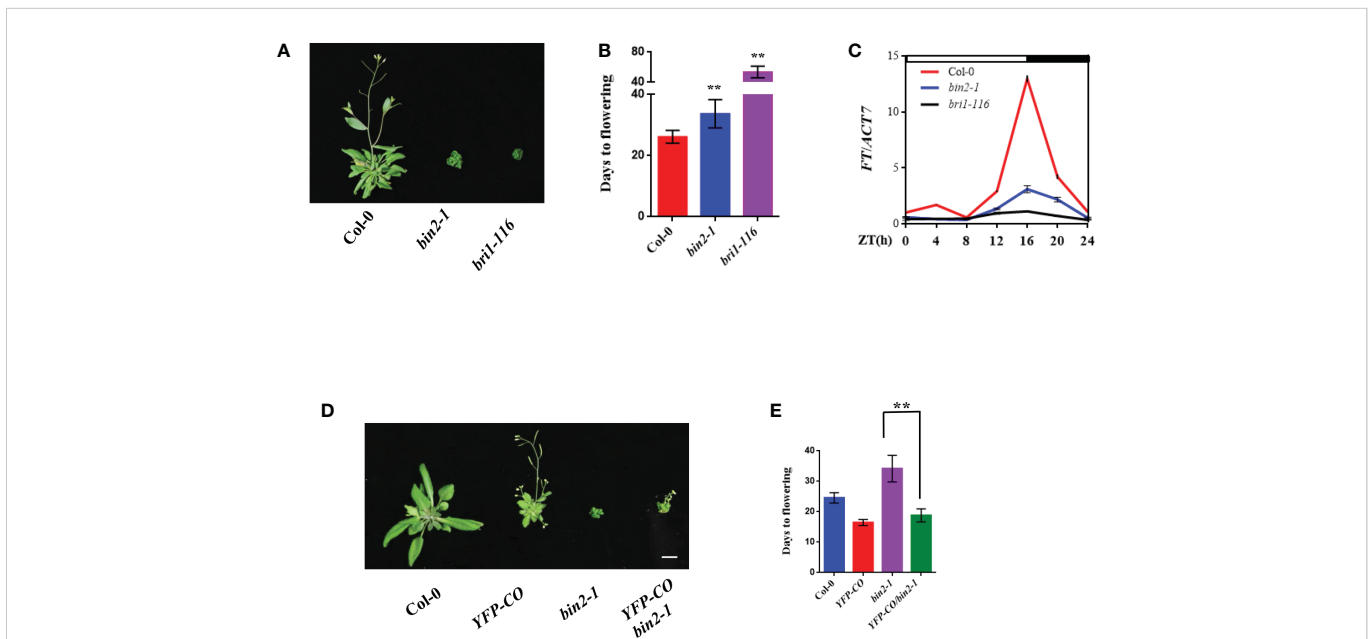

FIGURE 2
BR negatively regulates flowering time genetically upstream of CO. **(A)** Flowering phenotype of the indicated plants under LDs. Bar, 1 cm. **(B)** Days from germination to flowering of plants shown in **(A)**. Asterisks indicate a significant difference according to Student's t test (**, P <0.01), n > 20. **(C)** Diurnal expression pattern of *FT* in the indicated plants under LDs for 14 d. The mean values in Col-0 at Zeitgeber time (ZT) 0 were set to 1 (mean ± SD). White bars indicate day, and black bars represent night. **(D, E)** Genetic interaction assays between BIN2 and CO. Flowering phenotype of the indicated plants under LDs **(D)**. Days from germination to flowering of indicated plants **(E)**. Asterisks indicate a significant difference according to Student's t test (**, P <0.01), n > 20. Bar, 1 cm.

expression levels were largely abolished in the *bin2-1*, *det2-9* and *bri1-116* mutants (Figure 2C and Supplementary Figure 2C). These results imply that the late flowering phenotypes of these mutants were likely due to the down-regulation of *FT* transcription.

Considering that CO directly activates *FT* transcription (Onouchi et al., 2000; Samach et al., 2000), we were curious about the relationship between the BIN2 and CO in regulating flowering time. To this end, we studied the genetic interaction between BIN2 and CO. We generated the *CO*-overexpressing transgenic line *35S: YFP-CO* and introduced the *35S:YFP-CO* transgene into the *bin2-1* mutant background to generate the *35S:YFP-CO/bin2-1* lines. As shown in Figures 2D, E, the *35S:YFP-CO* transgenic line flowered much earlier than the wild type plant Col-0. Notably, the *35S:YFP-CO/bin2-1* line displayed obvious early-flowering phenotype compared with the *bin2-1* mutant, indicating that over expression of *CO* can rescue the late-flowering phenotype of *bin2-1* (Figures 2D, E). Consistent with the flowering phenotypes, the transcript levels of *FT* at ZT16 in *35S:YFP-CO/bin2-1* were higher than those in the *bin2-1* mutant (Supplementary Figure 3). This result demonstrates that BIN2 acts genetically upstream of CO in regulating flowering time.

BIN2 phosphorylates CO at the Thr280 residue

Since the protein kinase BIN2 interacts with CO, it is important to test whether CO is a substrate of BIN2. To this end, we used a phos-tag approach, where phosphorylated proteins in the gel containing phos-tag reagent are visualized as bands with slower migration compared with the corresponding dephosphorylated proteins. As shown in Figure 3A, the slower migrated band of CO could be observed when incubated with MBP-BIN2 and ATP; whereas this phenomenon could not be observed when incubated MBP-BIN2 without ATP (Figure 3A). These results demonstrate that BIN2 can phosphorylate CO. Consistently, the slower migrated band of CO was not observed when incubated with MBP-BIN2^{K69R} (the kinase dead

version of BIN2) and ATP (Figure 3A), suggesting that the kinase activity of BIN2 is required for the phosphorylation of CO.

In order to search for the putative phosphorylation sites of CO by BIN2, we first analyzed the putative BIN2 phosphorylation motifs in CO (Ser/Thr-X-X-X-Ser/Thr; Wang et al., 2002; Ryu et al., 2007; Ryu et al., 2010). As a result, we identified 13 putative phosphorylation motifs in CO protein (Supplementary Figure 4). Next, we mutated Ser/Thr to Ala in the 1th-3th phosphorylation motifs of CO (CO^{mN}), 4th-9th phosphorylation motifs of CO (CO^{mM}) and 10th-13th phosphorylation motifs of CO (CO^{mC}) to mimic non-phosphorylated forms of CO, respectively. As shown in Figure 3B, CO^{mN} and CO^{mM} was still phosphorylated by BIN2; in contrast, CO^{mC} was not phosphorylated by BIN2, illustrating that the phosphorylation sites are located in the 10th-13th phosphorylation motifs of CO (Figure 3B). Further, we mutated Ser/Thr to Ala in the 10th phosphorylation motifs of CO (CO^{mC-1}), 11th phosphorylation motifs of CO (CO^{mC-2}), 12th phosphorylation motifs of CO (CO^{mC-3}) and 13th phosphorylation motifs of CO (CO^{mC-4}), respectively. The results showed that the CO^{mC-1}, CO^{mC-2} and CO^{mC-4} mutant forms were still phosphorylated by BIN2; whereas CO^{mC-3} could not be phosphorylated, indicating that the phosphorylation sites are located at the 12th phosphorylation motif of CO (Figure 3C). Finally, we mutated the Thr280 and Thr284 residues at the 12th phosphorylation motif to Ala to generate the CO^{T280A} and CO^{T284A} mutant forms, respectively. As shown in Figure 3D, CO^{T284A}, but not CO^{T280A}, could be phosphorylated by BIN2, suggesting that the Thr280 residue is the specific BIN2 phosphorylation site of CO protein (Figure 3D). In summary, our efforts reveal that BIN2 can phosphorylate the Thr280 residue of CO protein.

Phosphorylation by BIN2 represses the function of CO in promoting flowering

To explore the biological relevance of CO phosphorylation by BIN2, we generated the *pCO : Flag-CO/co-9* and *pCO : Flag-CO^{T280A}/*
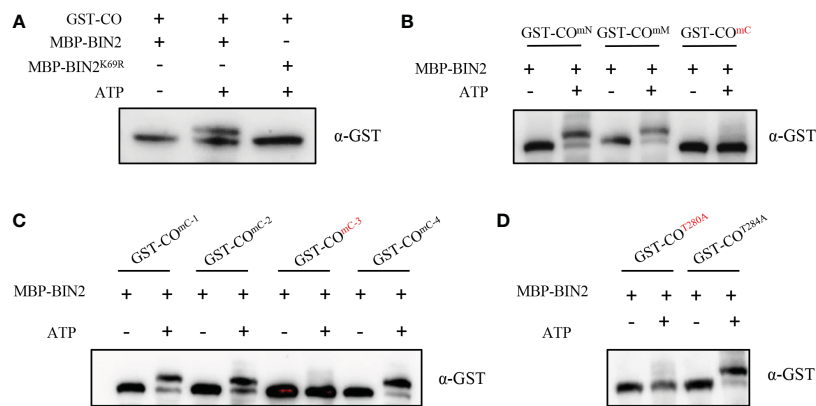

FIGURE 3
BIN2 phosphorylates CO. **(A)** Phosphorylation assays showing the BIN2-mediated phosphorylation of CO *in vitro*. Proteins were detected by immunoblotting with anti-GST antibody. **(B, C)** Phosphorylation assays showing the BIN2-mediated phosphorylation of CO with different mutant forms *in vitro*. Proteins were detected by immunoblotting with anti-GST antibody. **(D)** Phosphorylation assays showing the BIN2-mediated phosphorylation of CO^{T280A} and CO^{T284A}. Proteins were detected by immunoblotting with anti-GST antibody.

co-9 transgenic plants in the *co-9* mutant background. As shown in Figure 4A, the *pCO : Flag-CO* transgene could completely rescue the late-flowering phenotype of *co-9*. Notably, the *pCO : Flag-CO^{T280A}/co-9* lines flowered obviously earlier compared to *pCO : Flag-CO/co-9* and Col-0 (Figures 4A–C). The transcript levels of *CO* in these transgenic lines were comparable (Figure 4D). Consistent with the flowering phenotypes, the transcript levels of *FT* at ZT16 in the *Flag-*

COT280A/co-9 to *Flag-COT280A/co-9* plants were higher than those in the *pCO : Flag-CO/co-9* and Col-0 plants (Figure 4E). Then we checked whether the phosphorylation of CO affect the enrichments of CO on *FT*. To this end, we performed chromatin immunoprecipitation-quantitative PCR (ChIP-qPCR) assays using the 10-day-old *pCO : Flag-CO/co-9* and *pCO : Flag-COT280A/co-9* seedlings. As expected, in the *pCO : Flag-CO/co-9* transgenic plants, CO
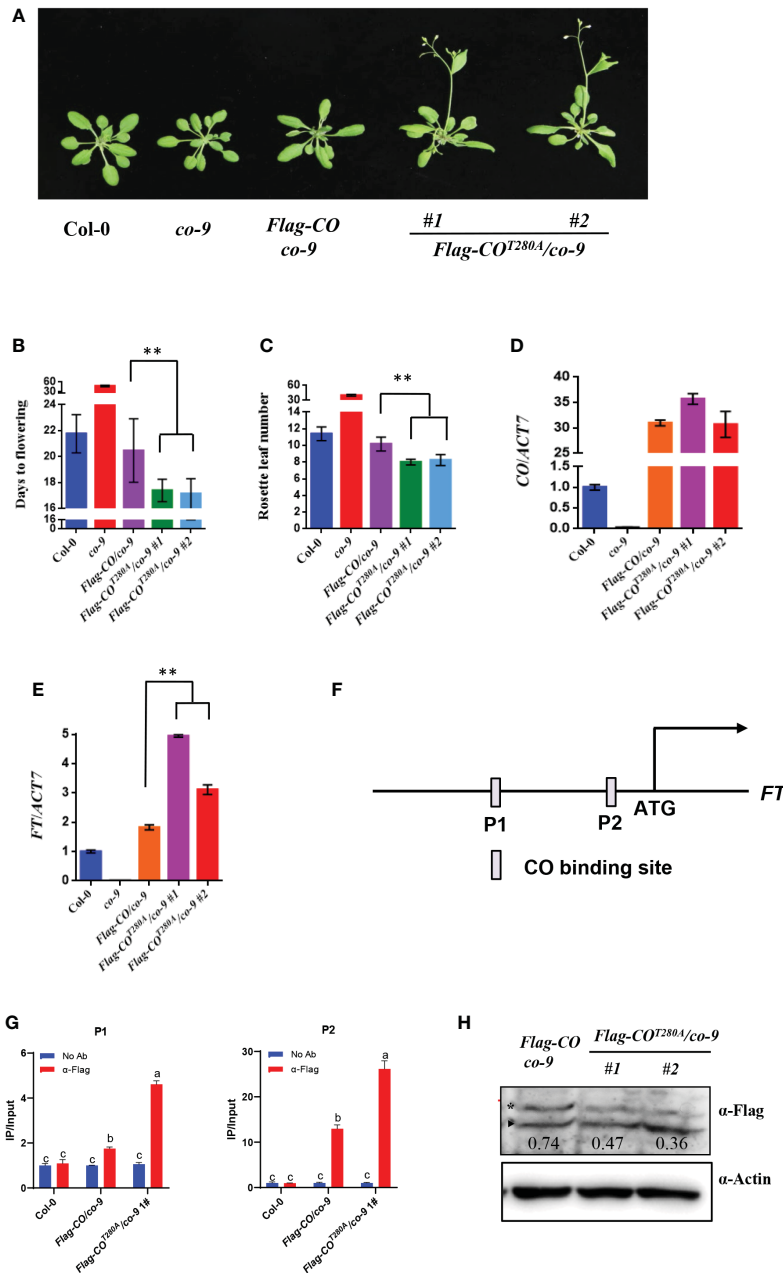

FIGURE 4
Phosphorylation of CO by BIN2 restricts its function in promoting flowering. **(A)** Flowering phenotype of the indicated plants under LDs. Bar, 1 cm.
(B) Days from germination to flowering of plants shown in **(A)**. Asterisks indicate a significant difference according to Student's *t* test (**, *P* <0.01), n > 20.
(C) Measurement of rosette leaf numbers of indicate a significant difference according to Student's *t* test (**, *P* < 0.01), n > 20. **(D, E)** qRT-PCR analysis showing the transcript levels of *FT* **(D)** and *CO* **(E)** at ZT16 in indicated plants under LDs. **(D, E)** qRT-PCR analysis showing the transcript levels of *CO* **(D)** and *FT* **(E)** at ZT16 in indicated plants under LDs. **(F)** Diagram depicting the putative promoter and genomic region of *FT*. **(G)** Representative results of the ChIP-qPCR assays. Chromatin fragments (~500 bp) were prepared from 10-day-old Col-0, *pCO : Flag-CO/co-9*, *pCO : Flag-COT280A/co-9* seedlings grown in LDs at ZT16. Immunoprecipitated by the anti-Flag antibody and the precipitated DNA was analyzed by qPCR using the primer pairs indicated. The IP/input ratios are shown with their SDs (n = 3). Different letters in the chart indicate statistically significant differences among different groups according to the one-way ANOVA analysis with Dunnett's multiple comparison test (P < 0.05). **(H)** The protein levels of CO at ZT16 in indicated plants under LDs. Flag-CO protein was detected by anti-Flag antibody. Actin was used as the loading control.

can directly bind to the promoters of *FT*. Meanwhile, the unphosphorylation of CO increased the enrichments of CO on *FT*, suggesting that the phosphorylation of CO inhibit the DNA-binding activity of CO to COREs in the *FT* promoter (Figures 4F, G). However, the CO protein levels were largely similar between the *pCO : Flag-CO^{T280A}/co-9* and *pCO : Flag-CO/co-9* transgenic plants (Figure 4H), illustrating that phosphorylation of CO by BIN2 does not influence CO protein stability. Next, we investigated whether the phosphorylation by BIN2 affects the interaction intensity between CO and TOE1/NF-YC4. The Y2H assays showed that the mutation of the Thr280 residue to Ala did not significantly affect the interaction intensity between CO and TOE1/NF-YC4 (Supplementary Figure 5). In addition, subcellular localization assay showed that the CO-YFP and CO^{T280A}-YFP

proteins were both localized in the nuclei, suggesting that the phosphorylation by BIN2 does not affect the subcellular localization of CO protein (Supplementary Figure 6). Taken together, these observations demonstrate that the phosphorylation of CO by BIN2 inhibits the function of CO in promoting flowering through affecting the DNA-binding activity of CO.

BIN2 represses the interaction of CO-CO

The formation of CO dimer/oligomer is possibly involved in influencing CO activity (Graeff et al., 2016; Lv et al., 2021). Here we showed that CO could interact with itself in plant cells (Figure 5A),
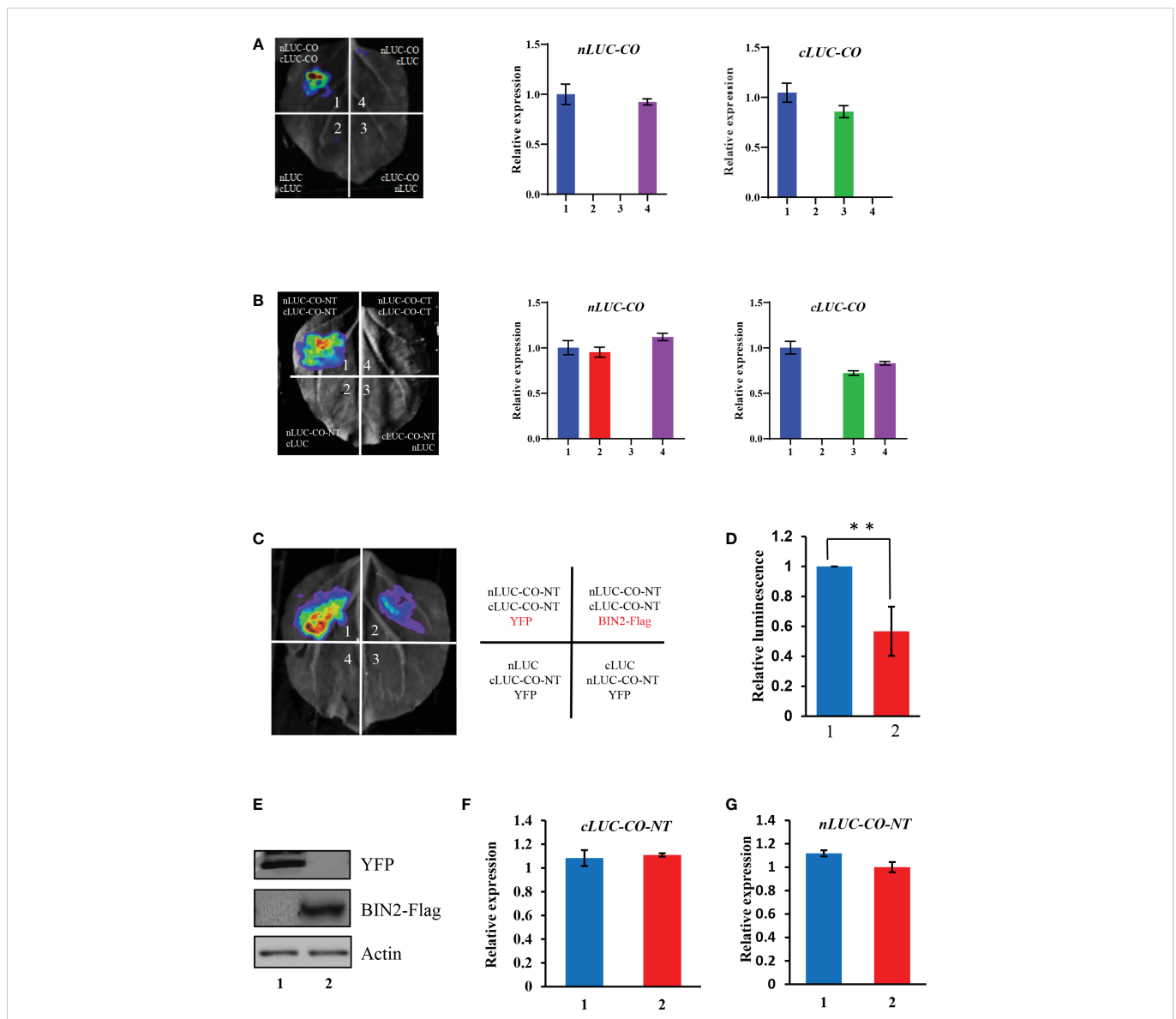

FIGURE 5
BIN2 represses CO-CO interaction. **(A)** LCI assays showing the interaction of CO-CO. The expression levels of *nLUC-CO* and *cLUC-CO* in the infiltrated *N. benthamiana* leaf areas were determined by qRT-PCR. Results were normalized to *NbACTIN1* (*NbACT1*). **(B)** LCI assays showing that the N-terminal part of CO mediates the interaction of CO-CO. The expression levels of *nLUC-CO* and *cLUC-CO* in the infiltrated *N. benthamiana* leaf areas were determined by qRT-PCR. Results were normalized to *NbACTIN1* (*NbACT1*). **(C, D)** LCI assays showing that BIN2 could inhibit the interaction of CO-CO. YFP was used as a control instead of BIN2-Flag. A representative image was shown in **(c)**, and the quantification of relative luminescence intensities was conducted in **(d)**. Data are means ± SD. Asterisks indicate a significant difference according to Student's *t* test (**, *P* <0.01). **(E)** Areas (infiltrations 1 and 2) were determined by immunoblotting. Actin was used as a loading control. **(F, G)** The transcript levels of *nLUC-CO* **(f)** and *cLUC-CO* **(g)** in the infiltrated *N. benthamiana* leaf areas (infiltrations 1 and 2) were quantified by qRT-PCR (means ± SD). Results were normalized to *NbACTIN1.*.

which may facilitate the formation of CO dimer/oligomer. Further, we conducted LCI assays to determine which region of CO is responsible for the interaction of CO-CO. The results showed that the N-terminal part of CO harboring the B-Box domain mediates the interaction of CO-CO (Figure 5B). As described above, the N-terminal part of CO also mediates the interaction of BIN2 and CO (Figure 1F). The findings that the B-Box domain of CO mediates the interaction of CO-CO prompted us to determine whether BIN2 competitively interferes with the CO-CO interaction. To test this idea, we co-expressed BIN2-Flag with nLUC-CO-NT and cLUC-CO-NT proteins in *N. benthamiana* leaves for LCI assays. The YFP protein was expressed instead of BIN2-Flag as a control. The results showed that the samples co-expressing nLUC-CO-NT/cLUC-CO-NT together with BIN2-Flag displayed weaker luminescence signals compared with those of samples co-expressing nLUC-CO-NT/cLUC-CO-NT and YFP (Figures 5C–G). Meanwhile, LCI assay showed that phosphorylation or unphosphorylation of CO did not significantly affect the interaction intensity between CO and CO (Supplementary Figure 7). These results demonstrate that BIN2 physically inhibits the interaction of CO-CO in plant cells.

Discussion

BR is involved in regulating floral transition. However, the underlying molecular mechanisms remain elusive. In this study, we showed that BR promotes flowering through inhibiting the function of CO *via* BIN2-mediated phosphorylation.

The protein kinase BIN2 is involved in several physiological processes by phosphorylating different transcription factors. For example, BIN2 phosphorylates BZR1/BES1 to promote their protein degradation and consequently represses BR signaling; BIN2 phosphorylates ICE1 to promote its degradation in response to cold stress; BIN2 phosphorylates and stabilizes RD26 and TINY to promote

drought stress response; BIN2 phosphorylates and stabilizes ABI5 to promote ABA response; BIN2 phosphorylates and inhibits SOS2 activity in regulating the salt stress response and growth recovery (He et al., 2002; Yin et al., 2002; Hu and Yu, 2014; Jiang et al., 2019; Xie et al., 2019; Ye et al., 2019; Li et al., 2020). On the other hand, a previous study reported that CO can be phosphorylated in planta (Sarid-Krebs et al., 2015). However, the protein kinases that phosphorylate CO remain to be identified. In this study, the phosphorylated band of CO protein can be clearly visualized; illustrating that CO can be phosphorylated by specific protein kinases. Here, we found that BIN2 physically interacts with CO *in vitro* and *in vivo* (Figures 1A–D). And the *bin2-1* mutant displayed obvious late-flowering phenotype and overexpression of *CO* could rescue the late-flowering phenotype of *bin2-1* (Figures 2D, E), suggesting that CO acts genetically downstream of BIN2. Next, we demonstrate that BIN2 phosphorylates the Thr280 residue of CO and restricts the function of CO in promoting flowering through affecting its DNA-binding activity. (Figures 4A–H). A recent study reported that SK12 negatively regulates flowering through interacting with and phosphorylating CO at threonine 119, thus facilitating CO degradation (Chen et al., 2020). These observations suggested that the different GSK3 protein kinases BIN2 and SK12 phosphorylate the Thr280 and Thr119 residues of CO, respectively, to restrict the its function.

In a recent study, structural analysis suggested that CO might form a homomultimeric assembly *via* its N-terminal B-Box domain and simultaneously occupy multiple cis-elements within the *FT* promoter (Lv et al., 2021). Here, we demonstrate that the N-terminal B-Box domain of CO is responsible for the interaction of both CO-CO and BIN2-CO (Figures 1F and 5B). Furthermore, we revealed that BIN2 competitively interferes with the CO(NT)-CO(NT) interaction that may facilitate the formation of CO dimer/oligomer (Figures 5C, D). Thereby, we propose that BIN2 phosphorylates CO to inhibit the DNA-binding activity and also prevents the interaction of CO-CO to restrict the function of CO in activating the transcription of *FT* transcription (Figure 6).
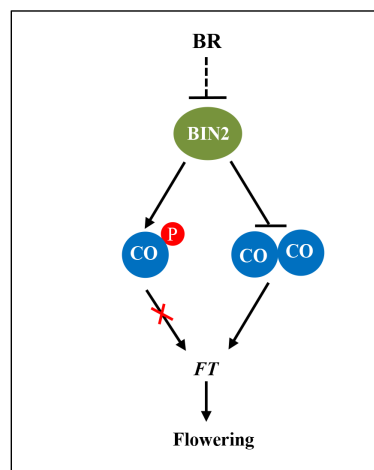

FIGURE 6
A propose working model for the regulation of CO activity by BIN2. The BR signaling repressor BIN2 physically interacts with and phosphorylates CO to inhibit the DNA-binding activity and also prevents the interaction of CO-CO to restrict the function of CO in activating *FT* transcription.

Data availability statement

Author contributions

Funding

Acknowledgments

Conflict of interest

Publisher's note

Supplementary material

References

Andrés, F., and Coupland, G. (2012). The genetic basis of flowering responses to seasonal cues. *Nat. Rev. Genet.* 13, 627–639. doi: 10.1038/nrg3291

Balasubramanian, S., Sureshkumar, S., Lempe, J., and Weigel, D. (2006). Potent induction of *Arabidopsis thaliana* flowering by elevated growth temperature. *PloS Genet.* 2, e106. doi: 10.1371/journal.pgen.0020106

Chaiwanon, J., Wang, W., Zhu, J. Y., Oh, E., and Wang, Z. Y. (2016). Information integration and communication in plant growth regulation. *Cell* 164, 1257–1268. doi: 10.1016/j.cell.2016.01.044

Chen, Y., Song, S. Y., Gan, Y. B., Jiang, L. X., Yu, H., and Shen, L. S. (2020). SHAGGY-like kinase 12 regulates flowering through mediating CONSTANS stability in *Arabidopsis*. *Sci. Adv.* 6, eaaw0413. doi: 10.1126/sciadv.aaw0413

Clough, S. J., and Bent, A. F. (1998). Floral dip: a simplified method for agrobacterium-mediated transformation of *Arabidopsis thaliana*. *Plant J.* 16, 735–743. doi: 10.1046/j.1365-313x.1998.00343.x

Clouse, S. D. (2008). The molecular intersection of brassinosteroid-regulated growth and flowering in *Arabidopsis*. *Proc. Natl. Acad. Sci. U. States America* 105, 7345–7346. doi: 10.1073/pnas.0803552105

Friedrichsen, D. M., Joazeiro, C. A., Li, J., Hunter, T., and Chory, J. (2000). Brassinosteroid-insensitive-1 is a ubiquitously expressed leucine-rich repeat receptor serine/threonine kinase. *Plant Physiol.* 123, 1247–1256. doi: 10.1104/pp.123.4.1247

Graeff, M., Straub, D., Eguen, T., Dolde, U., Rodrigues, V., Brandt, R., et al. (2016). MicroProtein-mediated recruitment of CONSTANS into a TOPLESS trimeric complex represses flowering in *Arabidopsis*. *PloS Genet.* 12, e1005959. doi: 10.1371/journal.pgen.1005959

He, G., Liu, J., Dong, H., and Sun, J. (2019). The blue-light receptor CRY1 interacts with BZR1 and BIN2 to modulate the phosphorylation and nuclear function of BZR1 in repressing BR signaling in *Arabidopsis*. *Mol. Plant* 12, 689–703. doi: 10.1016/j.molp.2019.02.001

He, J., Gendron, J. M., Yang, Y., Li, J., and Wang, Z. Y. (2002). The GSK3-like kinase BIN2 phosphorylates and destabilizes BZR1, a positive regulator of the brassinosteroid signaling pathway in *Arabidopsis*. *Proc. Natl. Acad. Sci. U. States America* 99, 10185–10190. doi: 10.1073/pnas.152342599

Hung, F., Lai, Y., Wang, J., Feng, Y., Shih, Y., Chen, J., et al. (2021). The *Arabidopsis* histone demethylase JMJ28 regulates CONSTANS by interacting with FBH transcription factors. *Plant Cell* 33, 1196–1211. doi: 10.1093/plcell/koab014

Hu, Y., and Yu, D. (2014). BRASSINOSTEROID INSENSITIVE2 interacts with ABSCISIC ACID INSENSITIVE5 to mediate the antagonism of brassinosteroids to abscisic acid during seed germination in *Arabidopsis*. *Plant Cell* 26, 4394–4408. doi: 10.1105/tpc.114.130849

Ito, S., Song, Y. H., Josephson-Day, A. R., Miller, R. J., Breton, G., Olmstead, R. G., et al. (2012). FLOWERING BHLH transcriptional activators control expression of the photoperiodic flowering regulator CONSTANS in *Arabidopsis*. *Proc. Natl. Acad. Sci. U. States America* 109, 3582–3587. doi: 10.1073/pnas.1118876109

Jang, S., Marchal, V., Panigrahi, K. C., Wenkel, S., Soppe, W., Deng, X. W., et al. (2008). Arabidopsis COP1 shapes the temporal pattern of CO accumulation conferring a photoperiodic flowering response. *The EMBO Journal* 27, 1277–1288. doi: 10.1038/emboj.2008.68

Jiang, H., Tang, B., Xie, Z., Nolan, T., Ye, H., Song, G., et al. (2019). GSK3-like kinase BIN2 phosphorylates RD26 to potentiate drought signaling in *Arabidopsis*. *Plant J.* 100, 923–937. doi: 10.1111/tpj.14484

Kim, T. W., and Wang, Z. Y. (2010). Brassinosteroid signal transduction from receptor kinases to transcription factors. *Annu. Rev. Plant Biol.* 61, 681–704. doi: 10.1146/annurev.arplant.043008.092057

Kobayashi, Y., Kaya, H., Goto, K., Iwabuchi, M., and Araki, T. (1999). A pair of related genes with antagonistic roles in mediating flowering signals. *Science* 286, 1960–1962. doi: 10.1126/science.286.5446.1960

Komeda, Y. (2004). Genetic regulation of time to flower in *Arabidopsis thaliana*. *Annu. Rev. Plant Biol.* 55, 521–535. doi: 10.1146/annurev.arplant.55.031903.141644

Kumimoto, R. W., Zhang, Y., Siefers, N., and Holt, B. F. (2010). NF-YC3, NF-YC4 and NF-YC9 are required for CONSTANS-mediated, photoperiod-dependent flowering in *Arabidopsis thaliana*. *Plant J.* 63, 379–391. doi: 10.1111/j.1365-313X.2010.04247

Li, T., Lei, W., He, R., Tang, X., Han, J., and Zou, L. (2020). Brassinosteroids regulate root meristem development by mediating BIN2-UPB1 module in *Arabidopsis*. *PloS Genet.* 16, e1008883. doi: 10.1371/journal.pgen.1008883

Li, J., Li, Y., Chen, S., and An, L. (2010). Involvement of brassinosteroid signals in the floral-induction network of *Arabidopsis*. *J. Exp. Bot.* 61, 4221–4230. doi: 10.1093/jxb/erq241

Li, J., and Nam, K. H. (2002). Regulation of brassinosteroid signaling by a GSK3/SHAGGY-like kinase. *Science* 295, 1299–1301. doi: 10.1126/science.1065769

Li, J., Nam, K. H., Vafeados, D., and Chory, J. (2002). *BIN2*, a new brassinosteroid-insensitive locus in *Arabidposis*. *Plant Physiol.* 127, 14–22. doi: 10.1104/pp.127.1.14

Liu, J., Cheng, X., Liu, P., Li, D., Chen, T., Gu, X., et al. (2017). MicroRNA319-regulated TCPs interact with FBHs and PFT1 to activate *CO* transcription and control flowering time in *Arabidopsis*. *PloS Genet.* 13, e1006833. doi: 10.1371/journal.pgen.1006833

Liu, L., Zhang, Y., Li, Q., Sang, Y., Mao, J., and Lian, H. (2008). COP1-mediated ubiquitination of CONSTANS is implicated in cryptochrome regulation of flowering in *Arabidopsis*. *Plant Cell* 20, 292–306. doi: 10.1105/tpc.107.057281

Lv, B., Tian, H., Zhang, F., Liu, J., Lu, S., Bai, M., et al. (2018). Brassinosteroids regulate root growth by controlling reactive oxygen species homeostasis and dual effect on ethylene synthesis in *Arabidopsis*. *PloS Genet.* 14, e1007144. doi: 10.1371/journal.pgen.1007144

Lv, X., Zeng, X., Hu, H., Chen, L., Zhang, F., Liu, R., et al. (2021). Structural insights into the multivalent binding of the *Arabidopsis FLOWERING LOCUS t* promoter by the CO-NF-Y master transcription factor complex. *Plant Cell* 33, 1182–1195. doi: 10.1093/plcell/koab016

Onouchi, H., Igeño, M. I., Périlleux, C., Graves, K., and Coupland, G. (2000). Mutagenesis of plants overexpressing CONSTANS demonstrates novel interactions among *Arabidopsis* flowering-time genes. *Plant Cell* 12, 885–900. doi: 10.1105/tpc.12.6.885

Putterill, J., Robson, F., Lee, K., Simon, R., and Coupland, G. (1995). The *CONSTANS* gene of *Arabidopsis* promotes flowering and encodes a protein showing similarities to zinc finger transcription factors. *Cell* 80, 847–857. doi: 10.1016/0092-8674(95)90288-0

Ryu, H., Kim, K., Cho, H., Park, J., Choe, S., Hwang, I., et al (2007). Nucleocytoplasmic shuttling of BZR1 mediated by phosphorylation is essential in Arabidopsis brassinosteroid signaling. *Plant Cell* 19, 2749–2762. doi: 10.1105/tpc.107.053728.

Ryu, H., Cho, H., Kim, K., and Hwang, I. (2010). Phosphorylation dependent nucleocytoplasmic shuttling of BES1 is a key regulatory event in brassinosteroid signaling. *Molecules and Cells* 29, 283–290. doi: 10.1007/s10059-010-0035-x

Samach, A., Onouchi, H., Gold, S. E., Ditta, G. S., Schwarz-Sommer, Z., Yanofsky, M. F., et al. (2000). Distinct roles of CONSTANS target genes in reproductive development of *Arabidopsis*. *Science* 288, 1613–1616. doi: 10.1126/science

Sarid-Krebs, L., Panigrahi, K. C., Fornara, F., Takahashi, Y., Hayama, R., Jang, S., et al. (2015). Phosphorylation of CONSTANS and its COP1-dependent degradation during photoperiodic flowering of *Arabidopsis*. *Plant J.* 84, 451–463. doi: 10.1111/tpj.13022

Sawa, M., Nusinow, D. A., Kay, S. A., and Imaizumi, T. (2007). FKF1 and GIGANTEA complex formation is required for day-length measurement in *Arabidopsis*. *Science* 318, 261–265. doi: 10.1126/science.1146994

Sun, J., Qi, L., Li, Y., Zhai, Q., and Li, C. (2013). PIF4 and PIF5 transcription factors link blue light and auxin to regulate the phototropic response in *Arabidopsis*. *Plant Cell* 25, 2102–2114. doi: 10.1105/tpc.113.112417

Tiwari, S. B., Shen, Y., Chang, H. C., Hou, Y., Harris, A., Ma, S. F., et al. (2010). The flowering time regulator CONSTANS is recruited to the *FLOWERING LOCUS t* promoter *via* a unique cis-element. *New Phytol.* 187, 57–66. doi: 10.1111/j.1469-8137.2010.03251.x

Turck, F., Fornara, F., and Coupland, G. (2008). Regulation and identity of florigen: *FLOWERING LOCUS t* moves center stage. *Annu. Rev. Plant Biol.* 59, 573–594. doi: 10.1146/annurev.arplant.59.032607.092755

Wang, Z., Bai, M., Oh, E., and Zhu, J. (2012). Brassinosteroid signaling network and regulation of photomorphogenesis. *Annu. Rev. Genet.* 46, 701–724. doi: 10.1146/annurev-genet-102209-163450

Wang, Z., Nakano, T., Gendron, J., He, J., Chen, M., Vafeados, D., et al. (2002). Nuclear-localized BZR1 mediates brassinosteroid-induced growth and feedback suppression of brassinosteroid biosynthesis. *Dev. Cell* 2, 505–513. doi: 10.1016/s1534-5807(02)00153-3

Xie, Z., Nolan, T., Jiang, H., Tang, B., Zhang, M., Li, Z., et al. (2019). The AP2/ERF transcription factor TINY modulates brassinosteroid-regulated plant growth and drought responses in *Arabidopsis*. *Plant Cell* 31, 1788–1806. doi: 10.1105/tpc.18.00918

Yang, Z., Yan, B., Dong, H., He, G., Zhou, Y., and Sun, J. (2021). BIC1 acts as a transcriptional coactivator to promote brassinosteroid signaling and plant growth. *EMBO J.* 40, e104615. doi: 10.15252/embj.2020104615

Yan, Z., Zhao, J., Peng, P., Chihara, R. K., and Li, J. (2009). BIN2 functions redundantly with other *Arabidopsis* GSK3-like kinases to regulate brassinosteroid signaling. *Plant Physiol.* 150, 710–721. doi: 10.1104/pp.109.138099

Ye, K., Li, H., Ding, Y., Shi, Y., Song, C., Gong, Z., et al. (2019). BRASSINOSTEROID-INSENSITIVE2 negatively regulates the stability of transcription factor ICE1 in response to cold stress in *Arabidopsis*. *Plant Cell* 31, 2682–2696. doi: 10.1105/tpc.19.00058

Yin, Y., Wang, Z., Mora-Garcia, S., Li, J., Yoshida, S., Asami, T., et al. (2002). BES1 accumulates in the nucleus in response to brassinosteroids to regulate gene expression and promote stem elongation. *Cell* 109, 181–191. doi: 10.1016/s0092-8674(02)00721-3

Zhang, B., Wang, L., Zeng, L., Zhang, C., and Ma, H. (2015). *Arabidopsis* TOE proteins convey a photoperiodic signal to antagonize CONSTANS and regulate flowering time. genes &. *Development* 29, 975–987. doi: 10.1101/gad.251520.114

Zheng, L., Baumann, U., and Reymond, J. L. (2004). An efficient one-step site-directed and site-saturation mutagenesis protocol. *Nucleic Acids Res.* 32, e11. doi: 10.1093/nar/gnh110